

Design of a Four-Rotor Aerial Robot

P. Pounds & R. Mahony
Department of Engineering
Faculty of Engineering and
Information Technology,
Australian National University,
ACT 0200.
mahony@ieee.org

P. Hynes & J. Roberts
CSIRO Manufacturing & Infrastructure
Technology,
Queensland Centre for Advanced Technology,
Pullenvale, QLD 4069
jonathan.roberts@csiro.au

Abstract

The design and fabrication of a prototype four-rotor vertical take-off and landing (VTOL) aerial robot for use as indoor experimental robotics platform is presented. The flyer is termed an X4-flyer. A development of the dynamic model of the system is presented and a pilot augmentation control design is proposed.

1 Introduction

Recent advances in computer and sensing technology, and the associated reduction in cost of such systems, have made the development of commercial aerial robotic systems a possibility. Fixed-wing unmanned aerial aircraft have been in service for some years and are being used routinely for military and meteorological purposes. Autonomous VTOL (vertical take-off and landing) vehicles capable of quasi-stationary (hover and near hover) flight have also been considered in recent years [Amidi *et al.*, 1999; E. Frazzoli and Feron, 2000; Shakernia *et al.*, 1999; Saripalli *et al.*, 2002; Chahl and Srinivasan, 1999]. Significant research interest and energy has been directed towards the development of autonomous helicopters due to their high payload to power ratio. Helicopters, however, are extremely dangerous in practice due to the exposed rotor blades, and are only suitable for autonomous applications where there is no chance of unintended human-robot interaction. Very little has been done on the development of indoor aerial robotic platforms [Hamel *et al.*, 2002; Altug *et al.*, 2002]. Such platforms have considerable commercial potential for surveillance and inspection roles in dangerous or awkward environments. The small size, highly coupled dynamics and low cost implementation of indoor aerial robotic devices poses a number of significant challenges in both construction and control.

In this paper we discuss the design, fabrication, dynamic modelling and prototype control strategy for a four rotor vertical take-off and landing (VTOL) craft

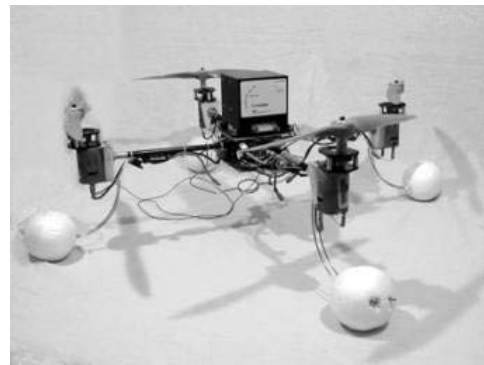


Figure 1: The X4-flyer developed in FEIT, ANU.

known as an *X4-flyer*. The design is specifically aimed at low cost simple and flexible implementation in a laboratory environment and several important design decisions follow from the clear goals of the project. The mechanical complexity of the device is deliberately kept to a minimum with no servo control systems or moving parts other than the rotors. The control system developed is a pilot augmentation system that will allow the craft to be flown by an experienced pilot.

2 Design and Fabrication

In this section we describe the physical components of the X4-flyer constructed.

2.1 Frame

The frame was required to be of a simple, rugged, demountable construction. A hub-and-spokes configuration was chosen to provide a simple demountable geometry. The spokes were constructed from 8.5mm diameter, 0.5mm thickness Cartel 'Hunter' 2117 shafts manufactured for hunting arrows. A bending strain analysis was undertaken to verify that the shafts would retain structural integrity even under extreme conditions. The hub was constructed from High-Density-Poly-Ethylene (HDPE) due to its high strength and suitability for shaping using standard tools. The hub

was designed as an under-over clamping system to provide a rugged demountable construction and preserve structural integrity of the frame struts. The struts are wrapped in gaff tape before the frame is clamped to prevent twisting and locating tabs were fitted to ensure the correct location and orientation of the struts on assembly.



Figure 2: The central hub construction of the X4.

Motor pods were constructed from an end fitted block of HDPE. A brass tube collar was manufactured to fix the end block to the strut. Landing gear was constructed from shaped bicycle spokes. The geometry of the landing gear was chosen to provide a spring force on the frame that will tend to right the craft in most moderate angle sliding impact conditions.

2.2 Motors and Rotors

The motor and rotor hardware was sourced from commercial RC equipment sold to hobby enthusiasts. The motors used were base level Johnson-683 500 series units typically used for RC racing cars. The speed controller used was an Rcline MSC-30B speed controller, a unit that weighs 26g and is rated to 30A at 12V. It is impossible to buy commercial rotors of a suitable dimension that are optimized for hover performance. Nevertheless, for the prototype project commercial RC aircraft rotors and gearing were used for reasons of simplicity and practicality. The use of rigid rotors simplifies the aerodynamic modelling and enhances control response, however, it also increases sensitivity to external disturbances and increases stresses on the frame of the robot (due to direct transmission of aerodynamic forces). The rotor used was an 11" diameter APC-C2 rotor with a 6" per revolution pitch along with a 2.9:1 gear system. Maximum thrust generated in static tests was $\approx 700\text{g}$. The figure of merit (cf. [Prouty, 1995]) calculation for the motor-rotor configuration used was 0.24. An ideal rotor has a figure of merit of 1 while a typical helicopter will have a figure of merit of around 0.6. There is considerable room for improvement of the performance of motor-rotor system with the purchase of quality motors and custom made rotors. In addition, the authors believe that a certain level of flexibility in the rotor will improve the controllability of the overall dynamic response despite an increase in complexity in aerodynamic modelling.



Figure 3: The motor/rotor unit for the X4.

2.3 Electronics and Control Logic

The principal goal of the prototype X4-flyer is to be used as an experimental platform in laboratory conditions. A key design principal was to program the control system architecture in SIMULINK on a ground based computer to allow quick and robust modification of control logic and dynamic control designs. Data communication was achieved using the serial communications protocol in RT-toolbox running in normal simulation mode within SIMULINK. At the discretization rate of 45Hz (determined by the sample rate of the RC-electronics) no significant problems with control system architecture was encountered.

An onboard processor is required to provide signal conditioning and management on board. An HC-12 single-board-computer (SBC) developed at QCAT was used as the onboard signal conditioning system. This card uses two HC-12 processors, outputs PWM signals that drive the speed controllers directly, inputs PWM signals from an R-700 JR Slimline RC receiver allowing direct pilot input from a JP X-3810 radio transmitter and has two separate RS232 serial channels, the first used to interface with the inertial measurement unit (IMU) and the second used as an asynchronous data link to the ground based computer. The HC-12 reads in the PWM input from the radio at 45Hz and the IMU data at 120Hz. Digital anti-aliasing filtering is applied to the IMU signals and they are down-sampled to 45Hz before all input data is transmitted to the ground based computer in asynchronous serial communication mode at 45Hz. The return control signals are received at a data rate of 45Hz and are converted into PWM signals and transmitted to the speed controllers.

An inertial measurement unit (IMU) is required to provide angular rate information and acceleration data. The most suitable unit considered was the EiMU (Embedded inertial Measurement Unit) developed by the robotics group in QCAT, CSIRO (cf. the unit is described in detail in [Roberts *et al.*, 2002]). This unit provides the required performance and weighs in the order of 50-100g. In the development of the prototype X4-flyer, QCAT provided a Crossbow DMU-6 unit on loan to Dep. Engineering. This unit weighs approximately 475g and severely compromised the performance of the prototype flyer.

2.4 X4-flyer

The complete flyer has a dry weight (excluding tether cables etc) of just less than 2kg. This weight includes the Crossbow DMU-6 unit. The calculated maximum thrust is in the order of 2.9kg indicating an acceptable thrust margin for manoeuvring. The overall dimension of the flyer is a frame length of 0.7m (excluding rotors) and a height of 0.24m.

In practice a truck battery was used for power supply and power tethers were required to supply current to the speed controllers. The additional weight of the tether along with a slight reduction in current due to internal battery resistance with all four motors drawing at the same time, lead to an increase in weight and a decrease in available lift. In experimental testing of the prototype X4-flyer, the thrust margin available for manoeuvring was insufficient and the experimental performance was unacceptable.

In the mark II prototype now under development the following key improvements will be made

1. The motor-rotor performance will be improved with a goal of a figure of merit of 0.4 or better. This will increase the available thrust to better than 4.5kg. Allowing a 30% thrust margin for manoeuvring the mission weight of the X4-flyer could be up to 3kg.
2. General weight savings in the flyer construction and components (particularly the IMU unit and the motors) will lead to a dry weight (without batteries or power tether) of less than 1.5kg. This will provide a potential payload of up to 1.5kg.
3. With the above weight savings the possibility of on board power supplies in the form of high performance rechargeable batteries will be investigated. A flight duration of two minutes would be acceptable.
4. The possibility of the addition of a wireless serial link will be investigated as well as the addition of a camera system that transmits video data to a base station over a wireless link.

3 Dynamic Model

The X4-flyer is configured with four counter-rotating rotors as shown in Figure 4.

Let $\mathcal{I} = \{E_x, E_y, E_z\}$ denote a right-hand inertial frame such that E_z denotes the vertical direction downwards into the earth. Let $\xi = (x, y, z)$ denote the origin of the body-fixed-frame $\mathcal{A} = \{E_1^a, E_2^a, E_3^a\}$, fixed at the centre of mass of the airframe. The orientation of the airframe is given by a rotation $R : \mathcal{A} \rightarrow \mathcal{I}$. Let $V \in \mathcal{A}$ denote the linear velocity and $\Omega \in \mathcal{A}$ denote the angular velocity of the airframe expressed in the body-fixed-frame. Let m denote the mass of the rigid object and let $\mathbf{I} \in \mathbb{R}^{3 \times 3}$ denote the constant inertia matrix around the centre of mass. Let T_H (total ‘heave’ thrust) and Γ denote the exogenous force and torque (respectively) applied to the flyer. Newton’s equations

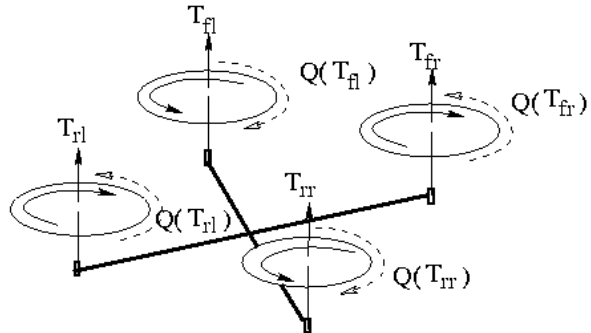


Figure 4: The force and torque inputs for an X4-flyer.

of motion yield the following dynamic model for the motion of the airframe:

$$\dot{\xi} = RV \quad (1)$$

$$m\dot{V} = -m\Omega \times V + mgR^T e_3 - T_H e_3 \quad (2)$$

$$\dot{R} = Rsk(\Omega), \quad (3)$$

$$\mathbf{I}\dot{\Omega} = -\Omega \times \mathbf{I}\Omega + \Gamma, \quad (4)$$

where g denotes acceleration due to gravity and e_3 denotes the unit vector with a one in the third entry. The notation $sk(\Omega)$ denotes the skew-symmetric matrix such that $sk(\Omega)v = \Omega \times v$ for the vector cross-product \times and any vector $v \in \mathbb{R}^3$. Note that the exogenous force is always applied in the vertical direction in the body fixed frame due to the rigid nature of the rotors.

The exogenous force and torque applied to the flyer are due to the aerodynamics and mechanical dynamics of the four rotors. Denote the rotors by the compass directions north, south, east and west respectively. The aerodynamic force generated by a rotor consists of a thrust T_i , $i \in \{N, S, E, W\}$, oriented along the linear axis of the rotor mast, and a drag Q_i acting around the rotor mast. Both the thrust and drag are proportional to the square of angular velocity of the rotor

$$T_i = \alpha\omega_i^2, \quad Q_i = \kappa\omega_i^2$$

for suitable proportionality constants κ and α . The dynamics of the i th DC-motor and rotor assembly is directly linked to the thrust via the proportional relation shown above. For the DC-motor itself, the dynamics between applied input to angular velocity of the shaft, can be approximated by a first order system

$$\begin{aligned} \dot{\omega}_i &= -\frac{1}{\tau} + \frac{K}{\tau}u_i - Q_i \\ &= -\frac{1}{\tau}\omega_i - \kappa\omega_i^2 + \frac{K}{\tau}u_i, \quad \omega_i \geq 0 \end{aligned}$$

where τ is the mechanical time-constant of the DC-motor (the electrical time-constant is an order of magnitude faster and may be ignored), K is the effective

gain of the system and the drag Q_i is the applied load due to air resistance. Note that the same system constants τ and K apply to all four motors. Substituting, for the thrust $T_i = \alpha\omega_i^2$ produces the input to thrust dynamics

$$\dot{T}_i = -\frac{2}{\tau}T_i - \frac{2\kappa}{\sqrt{\alpha}}T_i^{3/2} + \left(\frac{2\sqrt{\alpha}K}{\tau}\sqrt{T_i}\right)u_i \quad (5)$$

The rigid nature of the rotors considerably simplifies the physical modelling of the mechanical and aerodynamic properties of the rotors. There is a gyroscopic torque experienced by the rotor when the rotor mast moves with the body-fixed-frame angular velocity. The reaction torque applied to the airframe is

$$\Gamma_g = - \sum_{N,S,E,W} I_r(\Omega \times \pm(e_3\omega_i))$$

$$\Gamma_g(T_i, \Omega) = -\frac{I_r}{\sqrt{\alpha}} \sum_{N,S,E,W} (\Omega \times \pm e_3)\sqrt{T_i}$$

where I_r is the inertia of the rotor blade and the $\pm e_3$ vector is positive for the north-south rotors and negative for the counter-rotating east-west rotors. Finally, air velocity across the rotor plane causes a differential force between the advancing and receding blades of each rotor. Due to the rigid rotor assumption this results in a torque transmitted directly to the flyer frame

$$\Gamma_a = - \sum_{N,S,E,W} \gamma_a(V \times \pm(e_3\omega_i))$$

$$\Gamma_a(T_i, V) = -\frac{\gamma_a}{\sqrt{\alpha}} \sum_{N,S,E,W} (V \times \pm e_3)\sqrt{T_i}$$

where $\gamma_a > 0$ is a possibly large constant. The aerodynamic force considered is analogous to that responsible for rotor flapping in a helicopter and may only be tolerated on the X4-flyer due to the small diameter of the rotors used and quasi-stationary flight regimes considered. Despite the potentially large torques that are transmitted to the airframes due to the mechanical gyroscopic effects and the aerodynamic flapping torques these torques do not tend to effect the overall dynamic response of the system since in normal operating conditions $T_N \approx \dots \approx T_W$ and the contributions cancel out. It must be remembered that these contributions are still transmitted to the structural frame of the flyer.

If the composite exogenous forces applied to the flyer are written as a vector one has

$$\begin{pmatrix} \Gamma \\ T_H \end{pmatrix} = \begin{pmatrix} \Gamma_g(T_i, \Omega) + \Gamma_a(T_i, V) \\ 0 \end{pmatrix} +$$

$$\begin{pmatrix} 0 & 0 & d & -d \\ d & -d & 0 & 0 \\ (\kappa/\alpha) & (\kappa/\alpha) & -(\kappa/\alpha) & -(\kappa/\alpha) \\ 1 & 1 & 1 & 1 \end{pmatrix} \begin{pmatrix} T_N \\ T_S \\ T_E \\ T_W \end{pmatrix}$$

$$=: \Gamma_0(T_i, \Omega, V) + MT \quad (6)$$

where $d = 0.35\text{m}$ is the displacement of the rotors with respect to the center of mass of the X-4 flyer, Γ_0 is the

non-linear function modelling the combined mechanical gyroscopic and aerodynamic flapping torques experienced by the individual rotors, $T = (T_N, T_S, T_E, T_W)$ and M is the matrix defined by inspection.

The physical model of the system is given by the Newton-Euler equations (1-4), the thrust dynamics (5) for each individual motor and the force couple equations (6) showing how the various forces due to the rotors combine to generate the exogenous force inputs to the airframe rigid-body dynamics.

4 Linearization and Identification of the model

The physical model proposed in Section 3 for the X4-flyer is highly non-linear in character. Many of the non-linearities are second order effects and it is instructive to consider a linear approximation of the full model.

To obtain a linear parameterized model it is convenient to introduce Euler angles to represent the attitude of the airframe. The yaw-pitch-roll $\eta = (\phi, \theta, \psi)$ Euler angles¹ are used corresponding to aeronautical convention

$$R = \begin{pmatrix} c_\theta c_\phi & s_\psi s_\theta c_\phi - c_\psi s_\phi & c_\psi s_\theta c_\phi + s_\psi s_\phi \\ c_\theta s_\phi & s_\psi s_\theta s_\phi + c_\psi c_\phi & c_\psi s_\theta s_\phi - s_\psi c_\phi \\ -s_\theta & s_\psi c_\theta & c_\psi c_\theta \end{pmatrix}.$$

It is straight forward to derive the linearization of the Newton Euler equations around a hover conditions

$$\dot{\xi} = V \quad (7)$$

$$\dot{V} = \frac{g}{m} \begin{pmatrix} 0 & 1 & 0 \\ 0 & 0 & 1 \\ 0 & 0 & 0 \end{pmatrix} \eta \quad (8)$$

$$\dot{\eta} = \begin{pmatrix} 0 & 0 & 1 \\ 0 & 1 & 0 \\ 1 & 0 & 0 \end{pmatrix} \Omega \quad (9)$$

$$\dot{\Omega} = \Gamma^{-1} \begin{pmatrix} 0 & 0 & d & -d \\ d & -d & 0 & 0 \\ (\kappa/\alpha) & (\kappa/\alpha) & -(\kappa/\alpha) & -(\kappa/\alpha) \end{pmatrix} \begin{pmatrix} T_N \\ T_S \\ T_E \\ T_W \end{pmatrix} \quad (10)$$

The final line depends on all four inputs $\{T_N, T_S, T_E, T_W\}$ to control three dynamic states. The set point of the linearization condition imposes a further constraint

$$T_H = T_N + T_S + T_W + T_E = mg.$$

This constraint could be used to substitute for one of the thrust terms in Eq. 10. However, it is more convenient to introduce a further set of notations $\{T_R, T_P, T_Y\}$ to denote generalized roll, pitch and yaw forces. Define

$$T_R = d(T_W - T_E), \quad T_P = d(T_N - T_S)$$

$$T_Y = (\kappa/\alpha)(T_N + T_S - T_W - T_E)$$

¹These angles are sometimes termed the Z-Y-X Euler angles in Robotics texts.

The generalized input forces $\{T_H, T_R, T_P, T_Y\}$ (including heave) map into the actual rotor thrusts $\{T_N, T_S, T_E, T_W\}$ via the inverse of the matrix M defined in Eq. 6. By working with the generalized input forces the linear approximation decouples into two cascades of four integrators (governing motion in the (x, y) plane), null equations in the vertical direction since these dynamics are second order effects, and the yaw response

$$\begin{aligned}\dot{x} &= V_x, \quad \dot{V}_x = \frac{g}{m}\theta, \quad \dot{\theta} = \Omega_2, \quad \dot{\Omega}_2 = \frac{1}{\mathbf{I}_{22}} T_P \\ \dot{y} &= V_y, \quad \dot{V}_y = \frac{g}{m}\psi, \quad \dot{\psi} = \Omega_1, \quad \dot{\Omega}_1 = \frac{1}{\mathbf{I}_{11}} T_R \\ \dot{z} &= 0, \quad \dot{V}_z = 0, \\ \dot{\phi} &= \Omega_3, \quad \dot{\Omega}_3 = \frac{1}{\mathbf{I}_{33}} T_Y\end{aligned}$$

Finally, the motor dynamics of each individual rotor (Eq. 5) can be linearised around a set-point operating condition T_0

$$\dot{T}_i = -AT_i + Bu_i$$

where the constants A and B are related to the physical parameters of the system via

$$A = \left(\frac{2}{\tau} + \frac{3\kappa}{2\sqrt{\alpha}}\sqrt{T_0} \right), \quad B = \left(\frac{2\sqrt{\alpha}K}{\tau}\sqrt{T_0} \right)$$

The input signals $u = \{u_N, u_S, u_E, u_W\}$ are expressed in μs , the units of the PWM control signals. Note that

$$M^{-1} \begin{pmatrix} \dot{T}_N \\ \dot{T}_S \\ \dot{T}_E \\ \dot{T}_W \end{pmatrix} = -AM^{-1} \begin{pmatrix} T_N \\ T_S \\ T_E \\ T_W \end{pmatrix} + BM^{-1} \begin{pmatrix} u_N \\ u_S \\ u_E \\ u_W \end{pmatrix}$$

and defining new control inputs $v = \{v_H, v_R, v_P, v_Y\}$, by $v = M^{-1}(u_N, u_S, u_E, u_W)^T$ then one has

$$\dot{T}_i = -AT_i + Bv_i, \quad i = R, P, Y, H.$$

The control inputs v are used in the control design and are ‘mixed’ to produce the actual motor inputs u by the onboard processor.

The motor dynamics A and B were identified by running an open-loop experiment on a single motor attached to a custom made spring lever arm. It was necessary to include a time-lag of 0.022s in the motor dynamics that is due to the 45Hz discretization of the sampled-data control architecture. The airframe mass was measured directly in the lab and the inertia parameters were calculated based on a simplified point mass calculation. Non-dimensional thrust coefficients for both thrust and drag were measured in extensive experimental tests across a wide range of operating conditions. The proportional thrust and drag coefficients α and κ depend on local air-conditions and the non-dimensional thrust coefficients.

5 Control Design

The control problem considered was to develop a pilot augmentation control system. Such a system has the goal of modifying the dynamic response of the system in such a manner as to make it easily piloted by a competent pilot. The dynamic response of the system must be modified to conform to accepted dynamic performance of VTOL aircraft, however, it is not required to autonomously stabilize and control the vehicle. In a flight augmentation control system only the attitude dynamics need be considered.

The classical specifications of a pilot augmentation control system for pitch and roll performance are

System Type	Type I
Rise-time	$t_r < 1$ s
Settling time	$t_s < 5$ s
Damping ratio	$0.4 \leq \zeta \leq 1.3$

The dynamic model of the plant identified was

$$H_{\{P,R\}}(s) = \frac{27.5e^{-0.022s}}{s^2(s+4.1)}, \quad \{v_R, v_P\} \mapsto \{\theta, \psi\}$$

for the roll and pitch modes and

$$H_Y(s) = \frac{17.42e^{-0.022s}}{s^2(s+4.1)}, \quad \{v_Y\} \mapsto \{\theta, \psi\}$$

for the yaw mode. Note that the transfer functions considered are the linearization of the dynamics from the virtual control inputs v to the Euler-angles - not from the actual motor control inputs u . The two integrators at the origin correspond to the (undamped) rate dynamics and the angle kinematics.²

The control design undertaken consisted of an inner-outer loop architecture. Initially, the angular velocity in either pitch or roll is measured and used as a damping control input. A double lead compensator

$$C(s) = 2.4 \frac{53.5(s+3.7)(s+6.1)}{(s+34.8)(s+34.7)}$$

is proposed for the inner loop controller. The first lead compensator may be thought of as an approximate cancellation of the motor dynamics. The second lead compensator adds phase lead and improves the transient response dynamics to achieve the specified performance criteria with a proportional gain of 2.4. The inner-loop controller is designed to utilize up to 90% of the effective control margin available within the saturation levels of the PWM signals. Conceptually, 90% of the control effort is directed towards damping the high-frequency dynamics of the systems.

The outer loop design is a pure proportional feedback loop. The key idea was to keep this loop as simple as possible to avoid over-design of the control system.

²The rate dynamics will be lightly damped in practice, however, since rate gyros provide effective derivative feedback the inner-outer loop control architecture strongly augments any physical rate damping and it is not necessary to model its effects.

A proportional gain of 2 was sufficient to achieve the desired control specifications. It was verified that this gain specification would not lead to saturation of the control signal under normal operating requirements. The closed-loop time response of the nominal closed-loop system is shown in figure 5.

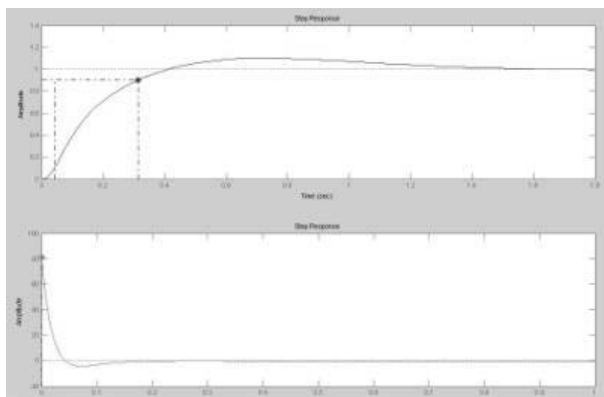


Figure 5: The simulated closed-loop time response to a pilot command step-input (above) and the demanded control effort (below).

In practice, the rate gyro measurement was easily obtained and (after a simple high-pass filter had been applied to cancel the sensor bias) provided good feedback control of the inner control loop. Accurate angle measurements are much more difficult to obtain. Since the flyer will accelerate laterally the moment that there is a slight inclination of the rotor plane, it is impossible to use the accelerometers to provide an estimate of the gravitational direction. A full filter of the system dynamics would need to be used and the angle estimate would, perforce, depend largely on the direct integration of the rate angles. The associated system was considered to complicated for the prototype control design and it was found that suitable control performance (for the pilot augmentation control system) was obtained using just the inner loop controller.

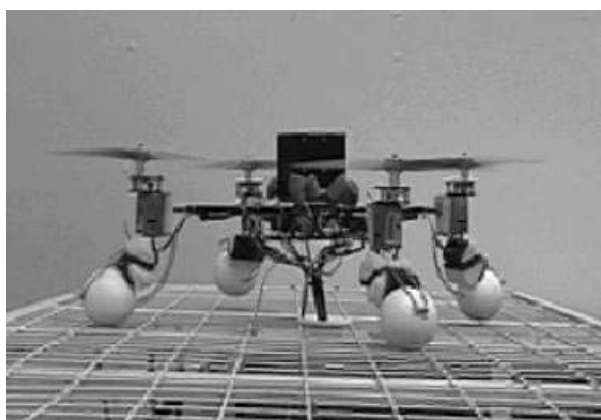


Figure 6: The X4-flyer 'almost' in flight.

Acknowledgments

The authors would like to acknowledge the contributions of all team members of the Queensland Centre for Advanced Technology robotics group in CSIRO Manufacturing & Infrastructure Technology.

References

- [Altug *et al.*, 2002] E. Altug, J. Ostrowski, and R. Mahony. Control of a quadrotor helicopter using visual feedback. In *Proceedings of the IEEE International Conference on Robotics and Automation, ICRA2002*, Washington DC, Virginia, USA, 2002.
- [Amidi *et al.*, 1999] O. Amidi, T. Kanade, and R. Miller. *Vision-based autonomous helicopter research at Carnegie Mellon robotics institute (1991-1998)*, chapter 15, pages 221–232. IEEE press and SPIE Optical Engineering press, New York, USA, 1999. Edited by M. Vincze and G. D. Hager.
- [Chahl and Srinivasan, 1999] J. Chahl and M. Srinivasan. Panoramic vision system for imaging, ranging and navigation in three dimensions. In *Proceedings of the International Conference on Field and Service Robotics, FSA '99*, Pittsburgh, Pennsylvania, USA., 1999.
- [E. Frazzoli and Feron, 2000] M. Dahlen E. Frazzoli and E. Feron. Trajectory tracking control design for autonomous helicopters using a backstepping algorithm. *Proceedings of the American Control Conference ACC*, pages 4102–4107, 2000.
- [Hamel *et al.*, 2002] T. Hamel, R. Mahony, R. Lozano, and J. Ostrowski. Dynamic modelling and configuration stabilization for an X4-flyer. In *Proceedings of the International Federation of Automatic Control Symposium, IFAC 2002*, Barcelona, Spain, 2002.
- [Prouty, 1995] Raymond W. Prouty. *Helicopter Performance, Stability and Control*. Krieger Publishing Company, 1995. reprint with additions, original edition 1986.
- [Roberts *et al.*, 2002] J. Roberts, P. Corkes, and G. Buskey. Low-cost flight control system for a small autonomous helicopter. In *Proceedings of the Australasian Conference on Robotics and Automation, ACRA02*, Auckland, New-Zealand, 2002.
- [Saripalli *et al.*, 2002] S. Saripalli, J.F. Montgomery, and G.S. Sakhatme. Vision based autonomous landing of an unmanned aerial vehicle. In *Proceedings of International Conference of Robotics and Automation, ICRA2002*, Wahsington DC, Virginia, USA, 2002.
- [Shakernia *et al.*, 1999] O. Shakernia, Y. Ma, T. J. Koo, and S. Sastry. Landing an unmanned air vehicle: vision based motion estimation and nonlinear control. *Asian Journal of Control*, 1(3):128–146, 1999.